Impact of Individual Defection on Collective Motion

Swadhin Agrawal[1], Jitesh Jhawar[2], Andreagiovanni Reina[3,4,5], Sujit P. Baliyarasimhuni[1], Heiko Hamann[3,4], and Liang Li[5,4,6]

[1] Department of Electrical Engineering and Computer Science, Indian Institute of Science Education and Research, Bhopal, India
`{swadhin20,sujit}@iiserb.ac.in`
[2] School of Arts and Sciences, Ahmedabad University, Ahmedabad, Gujarat, India
`jitesh.jhawar@ahduni.edu.in`
[3] Department of Computer and Information Science, University of Konstanz, Konstanz 78464, Germany
[4] Centre for the Advanced Study of Collective Behaviour, University of Konstanz, Konstanz 78464, Germany
[5] Department of Collective Behaviour, Max Planck Institute of Animal Behavior, Konstanz 78464, Germany
[6] Department of Biology, University of Konstanz, Konstanz 78464, Germany
`lli@ab.mpg.de`

Abstract. Collective motion modelling has attracted significant attention for gaining insights into the mechanisms of collective behaviour and its potential to inspire control strategies for swarm robotics. Most of the existing models assume that individuals within a group strictly adhere to the interaction rules. However, individuals in artificial and natural collectives could occasionally fail to follow the interaction rules, which is distinct from noisy actions. In this study, we analyse how the presence of individuals, who occasionally defect, affects the ordered phase of the group during collective motion. Using Monte Carlo simulations, we study two collective motion models, a non-spatial (pairwise interaction) and a spatial (Couzin) model. In the non-spatial model, when individuals defect with higher probability, both the time required by the agents to reach directional consensus (polarised group motion) as well as the average energy cost of the group to maintain such directional consensus (average rotational energy consumption per individual in highly polarised groups) increases. In the spatial model, there are conditions where the presence of defecting agents can simultaneously reduce the time required by the collective to get highly polarised and the average energy cost in the polarised state. These findings not only enhance our understanding of probabilistic defective behaviour in biological systems but can also inspire innovative, efficient, and controllable approaches in swarm robotics.

1   Introduction

Collective motion [46] is a universal phenomenon observed in nature, ranging from macro-molecules [39], to the simplest multicellular organisms [14], insects [37,7], fish [43], birds [4], herds [19], and even humans [34]. Over the past decades, mathematical models [38,45,13,24] have provided insights into how individuals, by interacting with their local neighbours, can collectively move in a coordinated manner. Most of these models assume that every individual adheres to the rules defined in these models with a certain degree of variability which is normally included as random noise. While individuals in natural systems, such as fish shoals or bird flocks, usually adhere to the interaction rules [4,25], they may also occasionally deviate from that behaviour in ways that are different from noisy actions. For instance, individuals may choose not to interact and instead take selfish actions to exploit collaboration efforts by their peers without paying relative social coordination costs [35,11]. Another reason why certain individuals may occasionally not follow the rules of collective motion is the fact that individuals have complex behaviours where collective motion is only one of its components. It is reasonable to assume that animals may concurrently forage, look for mates, or avoid dangers and predators; therefore, other individual goals than motion coordination could prevail in determining animals' actions [10,47,22,27,12]. Competition can also play a role in causing a temporary interruption in following collective motion rules [33,30]. We refer to the behaviour where individuals deviate from the collective motion rules as *defection*.

There are previous works that modelled intermittent, or occasional, defective behaviour in a variety of ways. Such studies considered variable frequencies of interaction, *i.e.*, agents always follow the cooperative rules, however, each of them has a personal frequency of interaction [6,16]. In such an asynchronous interaction system, certain agents update their behaviours (or states) more frequently than others. Slower agents (with lower interaction frequency) may appear as defectors to quicker agents that make (unilateral) updates of their behaviour without a direct response. Other studies considered individuals that selectively interact only with a subset of neighbours [23]. This research has provided interesting insights into the evolution of cooperation in collective systems [28,29]. Investigating the impact of occasional defection on collective motion remains an open question [2,48]. In this paper, we study whether having individuals with a given probability of defection (in our case, defection means ignoring the collective motion rule) can be beneficial for the group, and, if so, what level of defection maximises the collective benefits. Different from previous studies that used frequency-based or selective-interaction approaches to model defection at approximately regular time intervals [41,24], in our models, by introducing a probability for every agent to defect, we break the periodic patterns of defection events across the number of time steps.

Considering the impact of defecting agents in decentralised groups can also be relevant for the design of robotic systems, such as robot swarms [21]. While robots would be programmed to not defect and always follow the collaborative rules, their defective behaviour could be the consequence of malfunctioning or
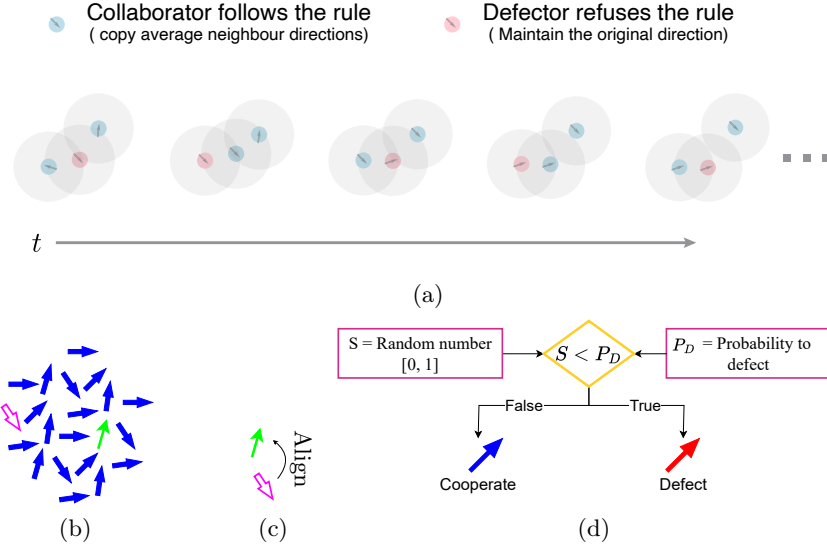
Fig. 1. (a) Illustration of the collective behaviour of individuals that probabilistically cooperate by following the collective motion rules or defect by maintaining their original directions. The pairwise model: (b) A pair of interacting agents in a group of fully connected agents, (c) Focal agents' (hollow pink) interaction rule, (d) Mechanism to update the agent's strategy (cooperate/defect) via the defection probability P_D.

noise. For instance, due to communication failures [31,17], noisy sensory inputs, and partial observability of the environment, robots may not always follow the prescribed algorithm [36]. Adversarial tampering is another example where the robot temporarily under the control of a hacker may behave erratically [3,26]. It is thus important to design algorithms that are robust to occasional defection by part of the robots, or that would even exploit defective behaviour to improve certain aspects of the group dynamics. This paper makes an initial step towards this research direction by analysing in what conditions probabilistic defection can improve or harm the group dynamics.

To do so, we analyse two prominent collective motion models, the pairwise model [24] (a non-spatial model) and the Couzin model [13] (a spatially-explicit model). We extend these two models to include the possibility that agents occasionally defect to investigate how this impacts the group dynamics. At each time step, an agent defects with probability P_D and otherwise cooperates by following the interaction rules. Figure 1(a) presents a schematic illustration of individuals defecting in the alignment interaction rule with probability $P_D = 1/3$. That is, an agent cooperates by aligning its orientation with its neighbours in two-thirds of the time steps and, instead, in the remaining one-third of time steps, it defects and maintains its original orientation, ignoring its neighbours. In this study, the agent's decision to cooperate or defect is independent of its neighbours' strategy and solely based on P_D, as illustrated in Fig. 1(d).

We measure the impact of defecting agents in terms of two metrics, polarisation time, T, and average energy cost, E, (defined in Sec.2). Polarisation time is the time the group needs to agree on the direction of motion, i.e., to have most of the agents aligned in the same direction. The average energy cost is the amount of energy the agents use to maintain a high level of polarisation (i.e., how much rotational energy each agent on average consumes to remain aligned in the same direction). For high levels of defection, the group may be unable to achieve a sufficient level of motion alignment, or the group may become polarised only for a short time before returning to a disordered state (unpolarised group).

In Sec. 3, we analyse the non-spatial pairwise model and observe that increasing defection probability P_D causes an increase in both polarisation time and average energy cost. In Sec. 4, we analyse the spatially-explicit Couzin model [13]. While the pairwise model only includes an alignment rule, the Couzin model is more complex as it comprises three rules. We find that when individuals defect in certain collective motion rules, as the defection probability increases (up to a certain point), both the polarisation time and average energy cost decrease. Note that, in this study, we do not compare the dynamics of the pairwise with those of the Couzin model since they are too different for a fair comparison, which is out of the scope of this study.

2   Methods

In the simulation, the agents move at a constant speed v. The kinematic motion of the agents is implemented using the Dubin's car model [15] described by

$$
\begin{aligned}
\dot{x} &= v \ \cos(\psi) \ , \\
\dot{y} &= v \ \sin(\psi) \ , \\
\dot{\psi} &= \omega \ .
\end{aligned}
\tag{1}
$$

Here, $\dot{x}$ and $\dot{y}$ are the velocities of the agent along each coordinate axis in the 2D plane, and ψ is the yaw (heading) angle of the agent. The turning rate ω, is constrained by a maximum of $\omega_{\max}$, i.e., $|\omega| < \omega_{\max}$. The desired turning rate for an individual is obtained from the interaction model (Secs. 3 and 4).

Given N agents in a group, we define the group polarisation $p(t)$ and the group energy cost $e(t)$ at a given time t. Group polarisation $p(t)$ is the average of the unit velocity vectors $\hat{\boldsymbol{v}}_i$ of individual agents i at time t, given by

$$
p(t) = \frac{|\sum\limits_{i=1}^{N} \hat{\boldsymbol{v}}_i(t)|}{N} \ ,
\tag{2}
$$

and group energy cost $e(t)$ at time t is measured as the sum of the rotational energy of each individual, given by

$$
e(t) = -\sum_{i=1}^{N} (\omega_i(t))^2 \ .
\tag{3}
$$

We perform Monte Carlo simulations [1,18], 100 independent runs for each condition (set of parameters). Each run lasts $t_{\max} = 200\,$s, with a time step $dt = 0.1$ sec. We measure the polarisation time T required to achieve a group polarisation $p(T)$ beyond a threshold value $p^* = 0.8$, $i.e.$ $p(T) > p^*$, and the average energy cost E per individual after the group gets polarised:

$$E = \frac{1}{N(t_{\max} - T)} \sum_{t=T}^{t_{\max}} e(t).$$ (4)

The agents move in an unbounded region and, at the start of each run, they are distributed uniformly at random inside a circular region of radius R_h with random heading angles. The initial states differed across the 100 different runs and across each model. In the case of the Couzin model, the same initial states were used across each type of defection.

3   Defection in the Pairwise Interaction Model

In the pairwise interaction model, the interaction network of the group is fully connected; hence, every agent can interact with any other agent. We use the same simulation algorithm of Jhawar et al. [24]. At each time step t, we chose at random $N/2$ agents as the focal agents that we pair with the rest of the group (non-focal agents). Each focal agent i (pink and hollow arrow in Fig. 1(b)) pairs with another unpaired agent j (thin and green quiver in Fig. 1(b)) chosen at random, irrespective of their Euclidean distance in space to copy $j's$ yaw angle, as shown in Fig. 1(c). Hence, only half of the population, the focal agent group, change its motion direction ($i.e.$, the rate of change of direction is 0.5, as in [24]). At every simulation step ($dt = 0.1$ s), the focal agents are re-sampled and paired with other random non-focal agents. Mathematically, the desired yaw for a focal agent is described by:

$$\psi_i(t+1) = \begin{cases} \psi_j(t), & \text{if cooperating} \\ \psi_i(t), & \text{if defecting} \end{cases}.$$ (5)

Hence, the turning rate of a focal agent is described by

$$\omega_i = \begin{cases} \min\left(\frac{\psi_i(t+1) - \psi_i(t)}{dt}, \omega_{\max}\right), & \text{if cooperating} \\ 0, & \text{if defecting} \end{cases}.$$ (6)

Under the above setup, we perform Monte Carlo simulations with $N = 50$ agents. We find that regardless of the defection probability value P_D, the group ultimately gets polarised ($i.e.$, $p(T) > p^*$), except when individuals always defect (hence, for $P_D = 1$ we do not compute polarisation time nor energy cost). Both polarisation time (Fig. 2(a)) and average energy cost per individual (Fig. 2(b)) increase with increasing P_D. Such an increase is much more pronounced for high defection probabilities, $i.e.$, $P_D > 0.7$.
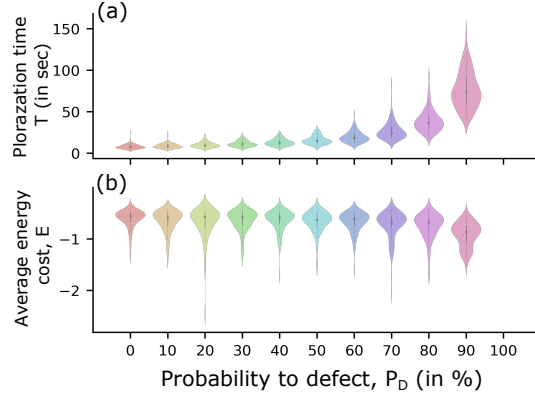
Fig. 2. (a) The polarisation time T and (b) the average energy cost E as a function of the probability to defect (P_D) in the pairwise model for $N = 50$ agents. The simulations were repeated 100 times per condition. We only report the data when at least 80% of the 100 simulation runs reached a polarisation greater than $p^* = 0.8$. Hence, data for $P_D = 1$ are omitted as the population does not reach polarisation.

4   Defection in the Couzin Model

In the Couzin model [13], an agent interacts with its neighbours within interaction range, therefore the interaction network results from Euclidean distances between agents. The interaction range is categorised into three zones: the zone of repulsion (Z_r), the zone of orientation (Z_o), and the zone of attraction (Z_a). Different physical distances and orientations from a focal individual define each of its zones, as shown in Fig. 3(a). When neighbours are present in the interaction zone, the focal agent interacts by getting attracted, repelled, or orienting towards its neighbours as long as they are not in the blind zone (α). In this model, at each simulation step $(dt = 0.1$ s), every agent acts as a focal agent and updates its yaw angle as a combination of the interactions in the three zones as:

$$\psi_i(t+1) = \begin{cases} \tan^{-1}\left(\frac{1}{N_r}\mathbf{d}_r^i(t)\right) & \text{if } Z_r^i \neq \phi \\ \tan^{-1}\left(\frac{1}{N_o}\mathbf{d}_o^i(t)\right) & \text{if only } Z_o^i \neq \phi \\ \tan^{-1}\left(\frac{1}{N_a}\mathbf{d}_a^i(t)\right) & \text{if only } Z_a^i \neq \phi \\ \tan^{-1}\left(\frac{1}{2}(\frac{1}{N_o}\mathbf{d}_o^i(t) + \frac{1}{N_a}\mathbf{d}_a^i(t))\right) & \text{if both } (Z_o^i, Z_a^i) \neq \phi \\ \psi_i(t) & \text{otherwise} \end{cases} \quad . \quad (7)$$

Here, $\mathbf{d}_r^i = -\sum_{j \in Z_r} \hat{\beta}_{ij}$, $\mathbf{d}_o^i = \sum_{j \in Z_o} \hat{v}_j$, and $\mathbf{d}_a^i = \sum_{j \in Z_a} \hat{\beta}_{ij}$, where the symbol $\hat{\beta}_{ij}$ represents a unit vector pointing from the position of focal agent i towards the position of the neighbour j (in the coordinate system of agent i). The symbols N_r, N_o and N_a represent the numbers of neighbours present in each zone $(Z_r,$

Z_o and Z_a, respectively). And $\hat{v}$ is a unit velocity vector. Hence, the desired ω_i of a focal agent at a given simulation step is obtained by:

$$\omega_i = \begin{cases} \min\left(\frac{\psi_i(t+1)-\psi_i(t)}{dt}, \omega_{\max}\right), & \text{if } i \text{ is cooperating} \\ 0, & \text{if } i \text{ is defecting} \end{cases}. \tag{8}$$

(a) Couzins model   (b) Cooperator (c) $D - Z_r$ (d) $D - Z_o$ (e) $D - Z_a$ (f) $D - Z_{\text{all}}$
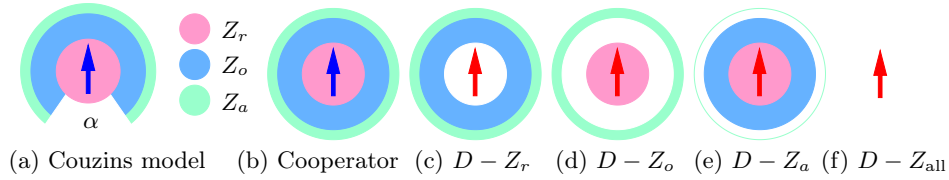
Fig. 3. (a) Focal agents' interaction zones in the Couzin model depicting the zone of orientation (Z_o), zone of attraction (Z_a), zone of repulsion (Z_r), and the blind region (α). Types of defection in the Couzin model: (b) standard Couzin model with repulsion, orientation, and attraction zones, (c-f) types of defection, white regions indicate no interaction (*i.e.*, defective interaction) for each interaction zone.

Given the modified Couzin model defined in Eqs.(7) and (8), we perform Monte Carlo simulations with $N = 20$ and $N = 50$ agents using similar parameter values to the ones used in the seminal work introducing the Couzin model [13], as indicated in Table 1 in detail. With more agents ($N \gg 50$) and the considered set of parameters (Table 1), the group takes longer than our simulation time of 200 seconds [9] to transit to the ordered phase, see supplementary [1] for the case of $N = 80$. In contrast to the pairwise model, we conduct Monte Carlo simulations by defining defection in four different ways based on the zones of behavioural interaction: (1) defection only in the zone of repulsion (D-Z_r, Fig. 3(c)), (2) defection only in the zone of orientation (D-Z_o, Fig. 3(d)), (3) defection only in the zone of attraction (D-Z_a, Fig. 3(e)), and (4) defection in all the three zones at the same time (D-Z_{all}, Fig. 3(f)).

Table 1. Parameters used in the Couzin model for highly parallel formation

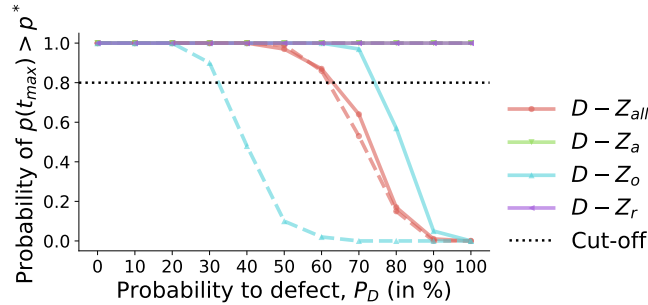| Parameter name	Symbol	Value	Unit
Radius of repulsion	R_r	1	units
Radius of orientation	R_o	18	units
Radius of attraction	R_a	20	units
Linear speed	v	5	units/s
Maximum turning rate	$\omega_{\max}$	$\pi/3$	rad/s
Field of invisibility	α	0	rad
Radius of home	R_h	$\sqrt{N}$	units

Fig. 4. Probability of having a polarised group (*i.e.*, $p(t_{\max}) > p^*$ with $p^* = 0.8$) as a function of the agent's probability P_D to defect. This probability is computed as the proportion of 100 simulation runs where, at time $t_{\max}$, the group had polarisation $p(t_{\max})$ above $p^* = 0.8$. The solid lines are for $N = 20$, and the dashed lines are for $N = 50$. In the results of Figs. 5 and 6, we do not include data for conditions where the probability of $p(t_{\max}) > p^*$ is below our cut-off line of 0.8 (dotted horizontal black line).

First, for each case of N ($N = 20$ and $N = 50$), we examine and report the probability of the group becoming highly polarised by the end of the experiment, *i.e.*, $p(t_{\max}) > p^*$. This probability is computed by computing the proportion of the 100 simulation runs (per condition) that are in a polarised state at time $t_{\max} = 200\,$s. The results in Fig. 4 show that in the case of defection of type $D - Z_r$ and $D - Z_a$, both groups of $N = 20$ and $N = 50$ agents consistently reach high polarisation levels irrespectively of the defection probability P_D, including the case of $P_D = 1$. However, in the case of $D - Z_{\text{all}}$, the probability of $p(t_{\max}) > p^*$ stays below our cut-off line set at 0.8 (horizontal dotted grey line) when defection probabilities are higher than $P_D > 0.6$ for both group sizes. In the case of $D - Z_o$, the system does not reliably reach a polarised state ($p(t_{\max}) < p^*$) in 200 seconds for $P_D > 0.7$ when $N = 20$ and $P_D > 0.3$ when $N = 50$. It means the collective ability to reach a polarised state with defection in zone Z_o decreases with an increasing number of agents.

Figures 5 and 6 show the results of the polarisation time T and the average energy cost E for simulations of groups of $N = 20$ and $N = 50$ agents, respectively. The analysis of these two metrics shows that there are large differences depending on the zone where agents probabilistically defect. For both group sizes, defection in the orientation zone Z_o leads to the negative effects of an increase in the polarisation time T and higher average energy costs E in maintaining a polarised state (see panels (e-f) of Figs. 5 and 6). We observe the opposite trend for defection in the repulsion zone Z_r (see panels (g-h) of Figs. 5 and 6, and Table 2) where, for both group sizes, the polarisation time T and average energy costs E decrease as the defection probability P_D increases. This trend is monotonic in all cases except for E with $N = 50$, where the minimum energy cost is for $P_D = 0.6$, see Fig. 6(h) and Table 2. For defection in the at-
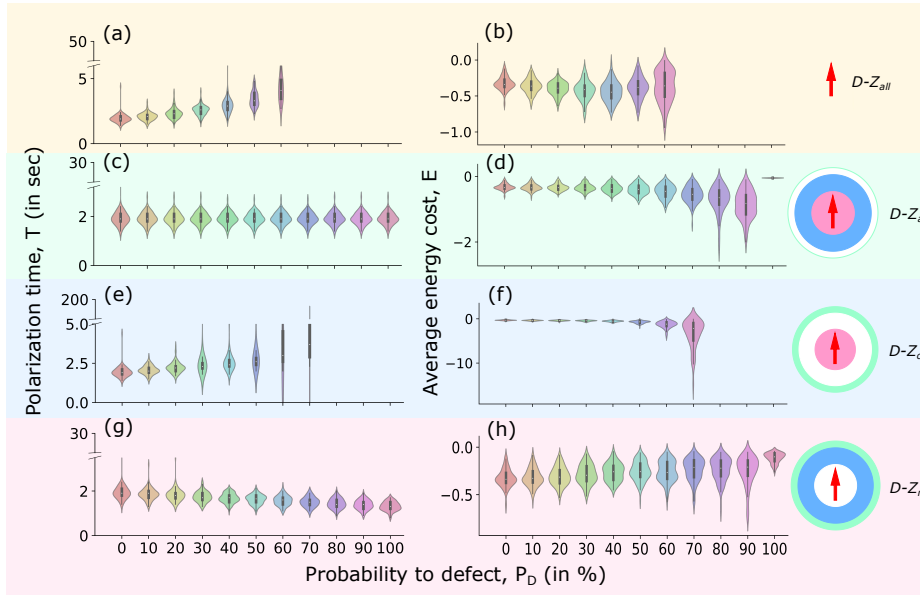
Fig. 5. The polarisation time T and the average energy cost E across four types of defection for a group of $N = 20$ agents. The violin plot shows the distribution of values from 100 simulation runs.

Table 2. Mean μ_e and standard deviation σ_e of the average energy cost E for $D - Z_r$, same data as in Fig. 6(h).

	0	10	20	30	40	50	60	70	80	90	100
μ_e	-3.109	-2.648	-2.234	-2.116	-1.877	-1.776	-1.697	-1.775	-2.140	-2.482	-0.595
σ_e	1.944	1.522	0.82	0.875	0.580	0.536	0.562	0.624	1.028	0.939	0.167

traction zone Z_a, we find different results for the two considered swarm sizes. In small swarms, $N = 20$ in Figs. 5(c-d), the inclusion of defection probability does not impact T but worsens average energy cost E. Instead, in larger swarms, $N = 50$ in Figs. 6(c-d), polarisation time T decreases for moderate values of defection probability $P_D \leq 0.3$ after plateauing at a constant T. Average energy cost E improves for $P_D < 0.3$, is minimum at $P_D = 0.3$, and increases for higher P_D (see Table 3). Finally, when agents defect in all three zones Z_{all}, the dynamics are quite complex as they are a combination of the trends we observed in the three areas. Polarisation time increases for $N = 20$ and has a minimum at $P_D = 0.3$ for $N = 50$ (see Fig. 6(a) and Table 4). Average energy cost E has opposite trends for $N = 20$ and $N = 50$. In the former case, Fig. 5(b) shows a u-shape trend, with a maximum energy cost for $P_D = 0.3$, and in the latter case, Fig. 6(b) shows a bell-shape trend with minimum energy cost for $P_D = 0.3$.
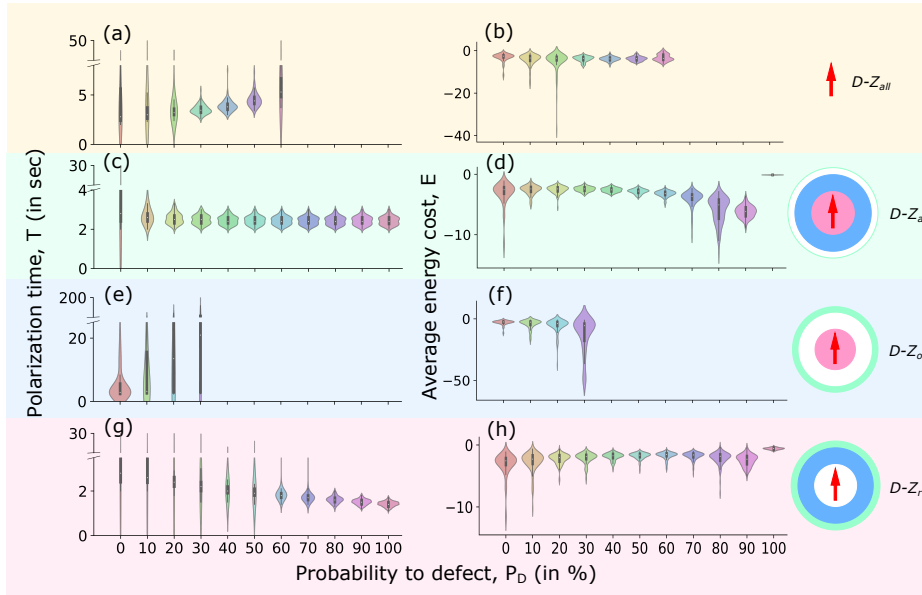
Fig. 6. The polarisation time T and the average energy cost E across four types of defection for a group of $N = 50$ agents. The violin plot shows the distribution of values from 100 simulation runs.

Table 3. Mean μ_e and standard deviation σ_e of the average energy cost E for $D - Z_a$, same data as in Fig. 6(d).

	0	10	20	30	40	50	60	70	80	90
μ_e	-3.109	-2.586	-2.538	-2.459	-2.595	-2.841	-3.235	-4.021	-5.891	-6.199
σ_e	1.944	0.769	0.59	0.391	0.371	0.404	0.51	1.294	2.129	0.993

Table 4. Mean μ_t and standard deviation σ_t of the polarisation time T for $D - Z_{all}$, same data as in Fig. 6(a).

	0	10	20	30	40	50	60
μ_t	5.501	4.773	3.665	3.522	3.877	4.564	7.408
σ_t	5.713	6.671	3.044	0.482	0.592	0.851	7.167

5   Conclusion

While most of the existing studies on collective motion models assume that individuals always obey the interaction rules without fail, in real-world natural and robotic systems agents may defect and not follow the interaction rules for various reasons, such as selfish behaviour, intra-group competitions, and adversarial attacks. In this paper, we introduce probabilistically defecting agents in two—non-spatial and spatial—models of collective motion: the pairwise model [24] and the Couzin model [13]. We analyse the impact of probabilistically defecting

agents on the collective motion dynamics by measuring the polarisation time T (time needed to reach polarisation $p(t)$ above $p^* = 0.8$, $p(T) > p^*$) and the average energy cost E per individual (energy that each agent spends on average to make rotational movements once the group has reached a highly polarised state).

Our analysis of the pairwise interaction model shows that both the polarisation time and the average group energy cost increase with increasing defection probability. The Couzin model is a spatial model thus we analysed four different types of defection depending on the region of space where agents occasionally defect. If agents defect in either the zone of attraction or repulsion, the polarisation time reduces with increasing defection probability P_D. With defection in these two zones, the average group energy cost E also has a minimum for defection probability $P_D > 0$. Differently, for defection in the zone of orientation, any value of $P_D > 0$ reduces the performance in terms of both polarisation time and average energy cost. In summary, in the considered spatial model (the Couzin model), there are conditions (*e.g.*, defection in the repulsion zone only) that can provide group-level benefits and conditions (*e.g.*, defection in the orientation zone only) that are harmful to the group. The system dynamics and their relationship with the investigated control parameters (defection probability, swarm size, defection zones) are relatively complex. Additional complexity is introduced in the spatial model by the possibility of agents splitting into subgroups moving in different directions with local polarisation in each subgroup.

Future research is needed to characterise better the causal relationship between defecting in certain zones and the resulting group dynamics, as well as how this potentially changes with the group size. For example, we hypothesise that measuring and controlling the density of defecting agents inside each interaction zone could give more insights into the observed dynamics or help explain the size-dependent dynamics for defectors in the zone orientation (Fig. 4). Future studies could also exploit the idea of using zone-selective probabilistic defection to improve the efficiency (polarisation speed and energy cost) of collective motion algorithms for robot swarms, or make the swarm's motion more robust against adversarial attacks [32,44]. Our long-term plans are to use the insights from this study to combine collective motion models with evolutionary games to understand the conditions where certain behavioural traits are likely to manifest, both at the group and individual levels (*e.g.*, splitting and merging of collectives [8], leader-follower [42,20,5] behaviour of individuals, and emergent leadership in groups [40]).

References

1. Agrawal, S., Jhawar, J., Reina, A., Baliyarasimhuni, S.P., Hamann, H., Li, L.: Supplementary materials of the article "Impact of individual defection on collective motion", https://github.com/swadhinagrawal/defectorsInCollectiveMotion.git
2. Antonioni, A., Cardillo, A.: Coevolution of synchronization and cooperation in costly networked interactions. Physical Review Letters **118**(23), 238301 (2017). https://doi.org/10.1103/physrevlett.118.238301
3. Aswale, A., López, A., Ammartayakun, A., Pinciroli, C.: Hacking the colony: On the disruptive effect of misleading pheromone and how to defend against it. In: Proceedings of the 21st International Conference on Autonomous Agents and Multiagent Systems. p. 27–34. AAMAS '22, International Foundation for Autonomous Agents and Multiagent Systems, Richland, SC (2022), https://dl.acm.org/doi/abs/10.5555/3535850.3535855
4. Ballerini, M., Cabibbo, N., Candelier, R., Cavagna, A., Cisbani, E., Giardina, I., Lecomte, V., Orlandi, A., Parisi, G., Procaccini, A., Viale, M., Zdravkovic, V.: Interaction ruling animal collective behavior depends on topological rather than metric distance: Evidence from a field study. Proceedings of the National Academy of Sciences **105**(4), 1232–1237 (2008). https://doi.org/10.1073/pnas.0711437105
5. Bernardi, S., Eftimie, R., Painter, K.J.: Leadership through influence: What mechanisms allow leaders to steer a swarm? Bulletin of Mathematical Biology **83**(6), 69 (2021). https://doi.org/10.1007/s11538-021-00901-8
6. Bode, N.W.F., Faria, J.J., Franks, D.W., Krause, J., Wood, A.J.: How perceived threat increases synchronization in collectively moving animal groups. Proceedings of the Royal Society B: Biological Sciences **277**(1697), 3065–3070 (2010). https://doi.org/10.1098/rspb.2010.0855
7. Buhl, J., Sumpter, D.J.T., Couzin, I.D., Hale, J.J., Despland, E., Miller, E.R., Simpson, S.J.: From disorder to order in marching locusts. Science **312**(5778), 1402–1406 (2006). https://doi.org/10.1126/science.1125142
8. Cardona, G.A., Leahy, K., Vasile, C.I.: Temporal logic swarm control with splitting and merging. In: 2023 IEEE International Conference on Robotics and Automation (ICRA). pp. 12423–12429. Piscataway, NJ (2023). https://doi.org/10.1109/ICRA48891.2023.10160335
9. Chazelle, B.: The convergence of bird flocking. Journal of the Association for Computing Machinery **61**(4) (2014). https://doi.org/10.1145/2629613
10. Collignon, B., Séguret, A., Chemtob, Y., Cazenille, L., Halloy, J.: Collective departures and leadership in zebrafish. PLoS ONE **14**(5), e0216798 (2019). https://doi.org/10.1371/journal.pone.0216798
11. Couzin, I.D.: Collective animal migration. Current Biology **28**(17), R976–R980 (2018). https://doi.org/10.1016/j.cub.2018.04.044
12. Couzin, I.D., Krause, J., Franks, N.R., Levin, S.A.: Effective leadership and decision-making in animal groups on the move. Nature 2004 433:7025 **433**(7025), 513–516 (2005). https://doi.org/10.1038/nature03236
13. Couzin, I.D., Krause, J., James, R., Ruxton, G.D., Franks, N.R.: Collective memory and spatial sorting in animal groups. Journal of Theoretical Biology (2002). https://doi.org/10.1006/jtbi.2002.3065
14. Davidescu, M.R., Romanczuk, P., Gregor, T., Couzin, I.D.: Growth produces coordination trade-offs in trichoplax adhaerens, an animal lacking a central nervous system. Proceedings of the National Academy of Sciences **120**(11), e2206163120 (2023). https://doi.org/10.1073/pnas.2206163120

15. Dubins, L.E.: On curves of minimal length with a constraint on average curvature, and with prescribed initial and terminal positions and tangents. American Journal of Mathematics **79**(3), 497–516 (1957), http://www.jstor.org/stable/2372560

16. Fatès, N.: A tutorial on elementary cellular automata with fully asynchronous updating. Natural Computing **19**(1), 179–197 (2020). https://doi.org/10.1007/s11047-020-09782-7

17. Gielis, J., Shankar, A., Prorok, A.: A critical review of communications in multi-robot systems. Current Robotics Reports **3**(4), 213–225 (2022). https://doi.org/10.1007/s43154-022-00090-9

18. Gillespie, D.T.: A general method for numerically simulating the stochastic time evolution of coupled chemical reactions. Journal of Computational Physics **22**(4), 403–434 (1976). https://doi.org/10.1016/0021-9991(76)90041-3

19. Gómez-Nava, L., Bon, R., Peruani, F.: Intermittent collective motion in sheep results from alternating the role of leader and follower. Nature Physics **18**(12), 1494–1501 (2022). https://doi.org/10.1038/s41567-022-01769-8

20. Goodrich, M.A., Pendleton, B., Baliyarasimhuni, S.P., Pinto, J.: Toward human interaction with bio-inspired robot teams. In: 2011 IEEE International Conference on Systems, Man, and Cybernetics. pp. 2859–2864. IEEE (2011). https://doi.org/10.1109/ICSMC.2011.6084115

21. Hamann, H.: Swarm robotics: A formal approach. Springer, Cham, Switzerland (2018). https://doi.org/10.1007/978-3-319-74528-2

22. Hensor, E., Godin, J.G., Hoare, D., Krause, J.: Effects of nutritional state on the shoaling tendency of banded killifish, fundulus diaphanus, in the field. Animal Behaviour **65**(4), 663–669 (2003). https://doi.org/10.1006/anbe.2003.2075

23. Jadhav, V., Guttal, V., Masila, D.R.: Randomness in the choice of neighbours promotes cohesion in mobile animal groups. Royal Society Open Science **9**(3), 220124 (2022). https://doi.org/10.1098/rsos.220124

24. Jhawar, J., Morris, R.G., Amith-Kumar, U.R., Danny Raj, M., Rogers, T., Rajendran, H., Guttal, V.: Noise-induced schooling of fish. Nature Physics **16**(4), 488–493 (2020). https://doi.org/10.1038/s41567-020-0787-y

25. Katz, Y., Tunstrøm, K., Ioannou, C.C., Huepe, C., Couzin, I.D.: Inferring the structure and dynamics of interactions in schooling fish. Proceedings of the National Academy of Sciences **108**(46), 18720–18725 (2011). https://doi.org/10.1073/pnas.1107583108

26. Kumar, Y., Paranjape, A.A., Ghosh, S., Baliyarasimhuni, S.P.: Adversarial fragmentation of robotic teams operating under reynolds' rules with bounded communication radius. In: 2023 62nd IEEE Conference on Decision and Control (CDC). pp. 2809–2814. IEEE (2023). https://doi.org/10.1109/CDC49753.2023.10383845

27. Leigh, E.G.: How does selection reconcile individual advantage with the good of the group? Proceedings of the National Academy of Sciences **74**(10), 4542–4546 (1977). https://doi.org/10.1073/pnas.74.10.4542

28. Li, A., Zhou, L., Su, Q., Cornelius, S.P., Liu, Y.Y., Wang, L., Levin, S.A.: Evolution of cooperation on temporal networks. Nature Communications **11**(1), 2259 (2020). https://doi.org/10.1038/s41467-020-16088-w

29. Li, L., Chen, C., Li, A.: Autonomy promotes the evolution of cooperation in prisoner's dilemma. Physical Review E **102** (2020). https://doi.org/10.1103/physreve.102.042402

30. MacGregor, H.E.A., Ioannou, C.C.: Collective motion diminishes, but variation between groups emerges, through time in fish shoals. Royal Society Open Science **8**(10), 210655 (2021). https://doi.org/10.1098/rsos.210655

31. Mayya, S., Egerstedt, M.: Safe open-loop strategies for handling intermittent communications in multi-robot systems. In: 2017 IEEE International Conference on Robotics and Automation (ICRA). pp. 5818–5823. Piscataway, NJ (2017). https://doi.org/10.1109/ICRA.2017.7989683

32. Mendívez Vásquez, B.L., Barca, J.C.: Adversarial scenarios for herding uavs and counter-swarm techniques. Robotica **41**(5), 1436–1451 (2023). https://doi.org/10.1017/S0263574722001801

33. Metcalfe, N.B., Thomson, B.C.: Fish recognize and prefer to shoal with poor competitors. Proceedings of the Royal Society of London. Series B: Biological Sciences **259**(1355), 207–210 (1995). https://doi.org/10.1098/rspb.1995.0030

34. Miller, N., Garnier, S., Hartnett, A.T., Couzin, I.D.: Both information and social cohesion determine collective decisions in animal groups. Proceedings of the National Academy of Sciences **110**(13), 5263–5268 (2013). https://doi.org/10.1073/pnas.1217513110

35. Moreira, J.A., Pacheco, J.M., Santos, F.C.: Evolution of collective action in adaptive social structures. Scientific Reports **3**, 1521 (2013). https://doi.org/10.1038/srep01521

36. Otterlo, M.v.: The Logic of Adaptive Behavior: Knowledge Representation and Algorithms for Adaptive Sequential Decision Making Under Uncertainty in First-order and Relational Domains. Frontiers in artificial intelligence and applications, IOS Press, Amsterdam, The Netherlands (2009)

37. Ramdya, P., Lichocki, P., Cruchet, S., Frisch, L., Tse, W., Floreano, D., Benton, R.: Mechanosensory interactions drive collective behaviour in drosophila. Nature **519**(7542), 233–236 (2015). https://doi.org/10.1038/nature14024

38. Reynolds, C.W.: Flocks, herds and schools: A distributed behavioral model. Computer Graphics **21**(4), 25–34 (1987). https://doi.org/10.1145/37402.37406

39. Schaller, V., Weber, C., Semmrich, C., Frey, E., Bausch, A.R.: Polar patterns of driven filaments. Nature **467**(7311), 73–77 (2010). https://doi.org/10.1038/nature09312

40. Strandburg-Peshkin, A., Papageorgiou, D., Crofoot, M.C., Farine, D.R.: Inferring influence and leadership in moving animal groups. Philosophical Transactions of the Royal Society B: Biological Sciences **373**(1746), 20170006 (2018). https://doi.org/10.1098/rstb.2017.0006

41. Strömbom, D., Hassan, T., Hunter Greis, W., Antia, A.: Asynchrony induces polarization in attraction-based models of collective motion. Royal Society Open Science **6**(4), 190381 (2019). https://doi.org/10.1098/rsos.190381

42. Tiwari, R., Jain, P., Butail, S., Baliyarasimhuni, S.P., Goodrich, M.A.: Effect of leader placement on robotic swarm control. In: Proceedings of the 16th Conference on Autonomous Agents and MultiAgent Systems. pp. 1387–1394. AAMAS '17, International Foundation for Autonomous Agents and Multiagent Systems, Richland, SC (2017). https://doi.org/https://dl.acm.org/doi/10.5555/3091125.3091316

43. Tunstrøm, K., Katz, Y., Ioannou, C.C., Huepe, C., Lutz, M.J., Couzin, I.D.: Collective states, multistability and transitional behavior in schooling fish. PLOS Computational Biology **9**(2), 1–11 (2013). https://doi.org/10.1371/journal.pcbi.1002915

44. Van Calck, L., Pacheco, A., Strobel, V., Dorigo, M., Reina, A.: A blockchain-based information market to incentivise cooperation in swarms of self-interested robots. Scientific Reports **13**, 20417 (2023). https://doi.org/10.1038/s41598-023-46238-1

45. Vicsek, T., Czirók, A., Ben-Jacob, E., Cohen, I., Shochet, O.: Novel type of phase transition in a system of self-driven particles. Physical Review Letters **75**(6), 1226–1229 (1995). https://doi.org/10.1103/physrevlett.75.1226

46. Vicsek, T., Zafeiris, A.: Collective motion. Physics Reports **517**(3), 71–140 (2012). https://doi.org/10.1016/j.physrep.2012.03.004
47. Yang, W.C., Schmickl, T.: Collective motion as an ultimate effect in crowded selfish herds. Scientific Reports **9**, 6618 (2019). https://doi.org/10.1038/s41598-019-43179-6
48. You, F., Yang, H.X., Li, Y., Du, W., Wang, G.: A modified vicsek model based on the evolutionary game. Applied Mathematics and Computation **438**, 127565 (2023). https://doi.org/10.1016/j.amc.2022.127565